Influence of carrier (polymer) type and drug-carrier ratio in the development of amorphous dispersions for solubility and permeability enhancement of ritonavir.

Pradip W. Dhore[a], Vivek S. Dave[b**], Suprit D. Saoji[a], Deepak Gupta[c], Nishikant A. Raut[a*]**

[a]Department of Pharmaceutical Sciences, R.T.M. Nagpur University, Nagpur, India
[b]St. John Fisher College, Wegmans School of Pharmacy, Rochester, NY, USA
[c]Lake Erie College of Osteopathic Medicine, School of Pharmacy, Bradenton, FL, USA

Received: May 11, 2017; *Accepted:* May 15, 2017

Original Article

ABSTRACT

The influence of the ratio of Eudragit® L100-55 or Kolliphor® P188 on the solubility, dissolution, and permeability of ritonavir was studied with a goal of preparing solid dispersions (SDs) of ritonavir. SDs were formulated using solvent evaporation or lyophilization techniques, and evaluated for their physical-chemical properties. The dissolution and permeability assessments of the functionality of the SDs were carried out. The preliminary functional stability of these formulations was assessed at accelerated storage conditions for a period of six months. Ritonavir: Eudragit® L100-55 (RE, 1:3) SD showed a 36-fold higher solubility of compared with pure ritonavir. Similarly, ritonavir:Kolliphor® P188 (RP, 1:2) SD exhibited a 49-fold higher solubility of ritonavir compared to pure ritonavir. Ritonavir dissolution from RE formulations increased with increasing ratios of Eudragit® L100-55, upto a ritonavir:carrier ratio of 1:3. The ritonavir dissolution from RP formulations was highest at a ritonavir:Kolliphor® P188 ratio of 1:2. Dissolution efficiencies of these formulations were found to be in line with, and supporting the dissolution results. The permeability of ritonavir across the biological membrane from the optimized formulations RE (1:3) and RP (1:2) were ~76 % and ~97 %, respectively; and were significantly higher compared to that of pure ritonavir (~20 %). A preliminary (six-month) stability study demonstrated the functional stability of prepared solid dispersions. The present study demonstrates that a good solubility, dissolution, and permeability improvement of ritonavir can be achieved with a careful choice of the carrier polymer, and by optimizing the amount of the chosen polymer in an SD formulation.

KEY WORDS: Ritonavir, solid-dispersion, solubility, dissolution, permeability

INTRODUCTION

Poor aqueous solubility, and rate-limited dissolution or absorption has resulted in low/variable bioavailability for most new drug molecules discovered using relatively modern approaches such as combinatorial chemistry and high throughput screening (1). Drugs developed by such methods possess requisite pharmacological properties, however, the efficacy of such drugs remains a matter of concern. Therefore, it becomes imperative to explore innovative formulation technologies to enhance the solubilization rate of drugs with

*Corresponding author: Nishikant A. Raut, Department of Pharmaceutical Sciences, Rashtrasant Tukadoji Maharaj Nagpur University, Nagpur, India, 440033, Tel: +91 942 280 3768, E-mail: nishikantraut29@gmail.com

** Both authors contributed equally

poor aqueous solubility for successful incorporation into orally bioavailable and therapeutically effective formulations (2, 3).

Several approaches for improving the solubility of such molecules have been explored previously (4). Formulating amorphous dispersions of such drugs, using one or more carrier polymers, is among the popular approaches used to improve the dissolution of poorly soluble drugs. Solid dispersions are uniform dispersions of one, or more, pharmacologically active molecule(s) in an inert carrier/matrix, usually prepared by techniques such as solvent-evaporation, melting, freeze-drying, spray-drying, etc. (5).

Ritonavir, a BCS class II drug (poor aqueous solubility/high permeability), is known to exhibit low/variable oral bioavailability (6). Published literature reports several approaches to improve the solubility/dissolution profile of ritonavir via formulating it into solid dispersions (7-9). However, most attempts of formulating solid dispersions of ritonavir have some lacunae. Law *et al.* prepared and evaluated ritonavir solid dispersions using polyethylene glycol (PEG 8000) as a carrier by solvent-evaporation and vacuum drying (8, 9). A major shortcoming of these studies is the use of high ritonavir:carrier ratio (1:9) with a ritonavir dose of 100 mg, resulting in a total mass of 1000 mg (excluding other excipients). The development of an oral solid dosage form with such a formulation will add to the bulk, making it an unfeasible endeavor. Sinha *et al.* attempted to overcome this issue by preparing solid dispersions of ritonavir using Gelucire® as a carrier polymer. This study was a relative improvement over the previous studies in that it used a ritonavir: carrier ratio of 1:4, and demonstrated an enhancement in the dissolution of ritonavir.

The presented study was initiated with a goal of exploring the feasibility of further reducing the amounts of carrier used to prepare solid dispersions of ritonavir, while increasing its solubility, dissolution, and permeability. Two polymers *viz.* Eudragit® L100-55 or Kolliphor® P188 were chosen as potential carrier-matrices in the formulation of ritonavir dispersions. Ritonavir is known to cause gastric acidity and abdominal pain (10). Eudragit® L100-55 is an enteric polymer known to promote drug solubilization and release at pH above 5.5 and would therefore be an appropriate choice as a carrier. Ritonavir is also infrequently associated with bleeding of the stomach or intestines (10). Kolliphor® P188 is reported to have an interesting and useful property of repairing damaged biological membranes (11, 12). Thus, considering the side effects of ritonavir and the reported beneficial properties of Kolliphor® P188, it was selected as another carrier matrix-former for the formulation of ritonavir dispersions.

The dispersions of ritonavir with Eudragit® L100-55 (RE) or Kolliphor® P188 (RP) were formulated using solvent evaporation or lyophilization methods. The prepared dispersions were initially characterized for their physical-chemical properties. This initial characterization of the dispersions was followed by an analysis of their functionality via dissolution and permeability analysis. Additionally, the influence of food on the functionality of the optimized formulations were evaluated via dissolution studies conducted under *fasted* and *fed* conditions. Finally, the functional stability of the optimized formulations assessed in a 180-day, controlled stability study.

MATERIALS AND METHODS

Materials

Ritonavir was obtained from Emcure Laboratories Pvt. Ltd., Pune, India. Eudragit® L100-55 was obtained from Evonik Degussa India Pvt. Ltd., Mumbai, India. Kolliphor® P188 was obtained from BASF India Ltd., Mumbai, India. 'Krebs solution' and the required dissolution media were prepared in the

laboratory. Analytical grade chemicals were used for all experiments.

Preparation of solid dispersions

Ritonavir-Eudragit® L 100-55 solid dispersion (RE)

Solid dispersions (RE) of ritonavir and Eudragit® L100-55 in different ratios (Table 1) were prepared using a solvent evaporation method described earlier by Tran *et al.* (13). Briefly, ritonavir and Eudragit® L100-55 were dissolved separately in ethanol, and the resulting solutions were mixed in a porcelain dish. This mixture was subjected to ultra-sonication (10 minutes) to ensure miscibility of both solutions. The solvent was evaporated by placing the mixture in an oven (50°C) for a period of 48 hours. The resulting solid dispersion (a thin, transparent film) was milled to a fine powder.

Ritonavir-Kolliphor® P188 solid dispersion (RP)

Solid dispersions (RP) of ritonavir and Kolliphor® P188 in different ratios (Table 1) were prepared using a freeze-drying technique reported earlier by Sonar *et al.* (14). Briefly, ritonavir and Kolliphor® P188 were dissolved separately in ethanol. The drug solution, and the polymer solution were blended in a porcelain dish. This mixture was subjected to ultra-sonication (10 minutes) to ensure that both solutions are homogeneously blended. The mixture was lyophilized at -50°C and 4000 mbar pressure using a bench-top freeze-dryer (Model: Lyodel, Delvac Pumps Pvt. Ltd., Chennai, India) for 24 hours. A uniform solid-dispersion powder was obtained after particle size reduction of the product obtained above.

Physical-chemical properties of the prepared dispersions

Solubility analysis

The saturation solubility of pure ritonavir and the prepared solid dispersions was carried out using a shake-flask technique reported earlier (4). Briefly, excess amount of ritonavir or the prepared solid-dispersion (~10 mg pure ritonavir) was placed in glass vials containing 10 ml of water (for RP), or phosphate buffer (pH-6.8 for RE). These test solutions were stirred (100 RPM) on a rotary shaker (Model: RS-24 BL, Remi Laboratory Instruments, Goregaon (E), Mumbai, India) at 37°C for 48 hours. Aliquots (5 ml) of samples were withdrawn at 48 hours, and filtered using a cellulose acetate filter (pore size 0.45 µM for ritonavir and 0.22 µM for the prepared dispersion, EMD Millipore®, Billerica, MA). The filtered samples, after suitable dilutions, were analyzed for ritonavir concentration at spectrophotometric wavelength of 239 nm.

Particle size and zeta potential analysis

The micromeritic properties of the dispersion samples was carried out using photon correlation spectroscopy on a laser diffraction particle size analyzer (Model: Nano Partica SZ-100, Horiba Instruments Pvt. Ltd., Singapore). The details of the procedure has been reported previously (7). The zeta potential for measuring the electrophoretic mobility of the prepared solid-dispersions was estimated using the Smoluchowski equation (15). Three independent sample replicates were used for all measurements.

Photomicroscopy

The morphology of pure ritonavir and the prepared solid-dispersions was primarily characterized by photomicroscopy. Briefly, a dispersion of pure ritonavir or the prepared solid-dispersions (~10 mg pure ritonavir) in 5 ml distilled water was prepared in glass vials. The aqueous dispersions were shaken gently, and the suspended particles were mounted on glass slides. The photomicrographs of the samples were captured with a microscope equipped with a digital camera (Model: DM 2500, Leica Microsystems, Germany).

Thermal analysis

The thermal behavior of pure ritonavir, Eudragit® L100-55, Kolliphor® P188, the physical mixtures of ritonavir with Eudragit® L100-55 or Kolliphor® P188, and the prepared solid dispersions was determined by differential scanning calorimetry (DSC). Procedural details of the preparation has been reported previously (16, 17).

Fourier-transform infrared (FTIR) spectroscopy

A FTIR spectrophotometer (Model: IR Prestige-21, Shimadzu, Japan) was used for the infrared spectral analysis of pure ritonavir, Eudragit® L100-55, Kolliphor® P188, the physical mixtures of ritonavir with Eudragit® L100-55 or Kolliphor® P188, and the prepared solid dispersions. All samples, before subjecting to FTIR analysis, were vacuum-dried to ensure removal of any residual moisture. 45 scans at a resolution of 4 cm^{-1} were carried out for each sample. The measurements were made in the wavelength range of 4000 to 600 cm^{-1}.

X-ray diffractometry

The crystal state analysis of the samples, i.e. pure ritonavir, Eudragit® L100-55, Kolliphor® P188, the physical mixtures of ritonavir with Eudragit® L100-55 or Kolliphor® P188, and the prepared solid dispersions were carried out on a powder x-ray diffractometer (Model: D8 Phaser, Bruker AXS, Inc., Madison, WI, USA). The details of the procedures have been published previously (7, 16).

Performance evaluation of the ritonavir dispersions

Ritonavir dissolution

The dissolution studies of pure ritonavir and the prepared solid-dispersions were conducted using a dissolution apparatus (USP Type II, paddle method, Model: TDT-08LX, Electrolab India Pvt. Ltd., Mumbai, India) equipped with Elab Disso Lite software, at 37°C and a stirring rate of 50 RPM. The dissolution medium for RE consisted of HCl (0.1N, pH-1.2) for the first two hours, followed by a phosphate buffer (0.05M, pH-6.8) for the remaining duration of the study. The dissolution medium for RP was phosphate buffer (0.05M, pH-6.8). Accurately weighed amounts of pure ritonavir (50 mg), or the prepared solid-dispersions (~50 mg ritonavir) were added to the dissolution media separately, and aliquots were withdrawn at predetermined intervals. The withdrawn samples were membrane-filtered (pore size 0.45 µM for ritonavir and 0.22 µM for the prepared dispersion) and after suitable dilutions, analyzed at a spectrophotometric wavelength of 239 nm against the blank.

To further analyze their dissolution performance, the dissolution efficiencies (DE) of pure ritonavir and the prepared solid-dispersions were computed and compared, using the dissolution results. The dissolution efficiencies were estimated using the relationship proposed by Anderson *et al.* (18)

Fasted versus fed state dissolution

The food effects on the absorption of ritonavir from the prepared solid-dispersions were evaluated in Fasted-State Simulated Intestinal Fluid (FaSSIF) and Fed-State Simulated Intestinal Fluid (FeSSIF) dissolution media. The details of the methods followed for the preparation of blank FaSSIF and FeSSIF media have been reported previously (19). The dissolution was carried out using a standard dissolution apparatus (USP type II, paddle method, Model: TDT- 08LX Electrolab India Pvt. Ltd., Mumbai, India) in FaSSIF (500 ml) or FeSSIF (1000 ml) media at 37 ± 0.5°C, using a stir rate of 50 RPM. Samples (5 ml) were withdrawn at 15 minute time intervals, membrane-filtered (pore size 0.45 µM for ritonavir and 0.22 µM for the prepared dispersion), and analyzed spectrophoto-

metrically at 251 nm (for FaSSIF), or 305 nm (for FeSSIF).

Ritonavir permeability

The ritonavir permeability from the prepared solid-dispersions was assessed using *everted* rat intestine technique as reported previously (7, 16, 20). The Institutional Animal Ethics Committee (IAEC) approved the use of experimental animals in the study. The permeability of ritonavir from the formulated solid dispersions was estimated by spectrophotometrically analyzing the samples collected every 15 minutes, at 239 nm.

Preliminary functional stability assessment

The functional stability of the optimized solid-dispersions was assessed by storing the samples for six months at accelerated conditions of temperature and humidity. The samples were stored at 25 ± 2ºC and 60 ± 5% RH. The formulations in tightly-closed, light-resistant high-density polyethylene (HDPE) vials were placed in controlled-conditions stability chambers for 180 days. At the end of storage, the samples were assessed for the dissolution and permeability of ritonavir (21-23).

RESULTS AND DISCUSSION

Physical-chemical properties of the prepared dispersions

Saturation solubility

The results of the aqueous solubilities of ritonavir alone and the formulated solid dispersions with Eudragit® L 100-55 (RE) or Kolliphor® P188 (RP) are shown in Table 1. Pure ritonavir was found to be practically insoluble in water (0.37 ± 0.03 µg/ml) or pH-6.8 phosphate buffer (0.39 ± 0.04 µg/ml). The solubility of ritonavir in RE solid-dispersion increased with the increasing Eudragit® L 100-55 ratio up to 1:3 (ritonavir:Eudragit® L 100-55). The optimized RE solid-dispersion demonstrated a significant increase (36-times) in the aqueous solubility of ritonavir. Similarly, the solubility of ritonavir in RP solid-dispersion increased with the increasing Kolliphor® P188 ratio upto 1:2 (ritonavir:Kolliphor® P188). This RP formulation showed a significant increase (49-fold) in the aqueous solubility of ritonavir. The observed increase in the solubility of ritonavir may be caused by a reduction in the molecular crystallinity (partial amorphization) of ritonavir in the prepared solid-dispersions (7).

Table 1 Saturation solubility of pure ritonavir, and ritonavir in the prepared solid dispersions

DRUG: CARRIER RATIO	RITONAVIR SOLUBILITY (µg/ml)*	
	RITONAVIR: EUDRAGIT® L 100-55 (in PBS pH 6.8)	RITONAVIR: KOLLIPHOR® P188 (in water)
Pure Ritonavir	0.39 ± 0.04	0.37 ± 0.03
1:1	7.54 ± 0.07	15.31 ± 0.07
1:2	12.16 ± 0.04	18.15 ± 0.09
1:3	14.09 ± 0.07	13.39 ± 0.04
1:4	10.81 ± 0.06	9.61 ± 0.07

*Values represent mean ± Std. Dev. (n=3)

Micromeritic properties of the prepared dispersions

Figure 1 shows the particle size distribution and zeta potential analysis of optimized RE (Figure 1A) and RP (Figure 1B). The mean particle size of the optimized RE (Figure 1Aa) solid dispersions was 305.6 ± 16.3 nm. The mean particle size of the optimized RP solid dispersions (Figure 1Ba) was observed to be 323.7 ± 17.6 nm. The surface area/volume (SA/V) ratio for most pharmaceutically processed materials is inversely proportional to their particle size (24). The small particle size of the optimized solid dispersions facilitates an easier release of the Active Pharmaceutical Ingredient (API) from the formulation via diffusion and/or surface erosion. Moreover, the smaller particle size of prepared solid dispersions also facilitates the transport across biological drug barriers (25, 26).

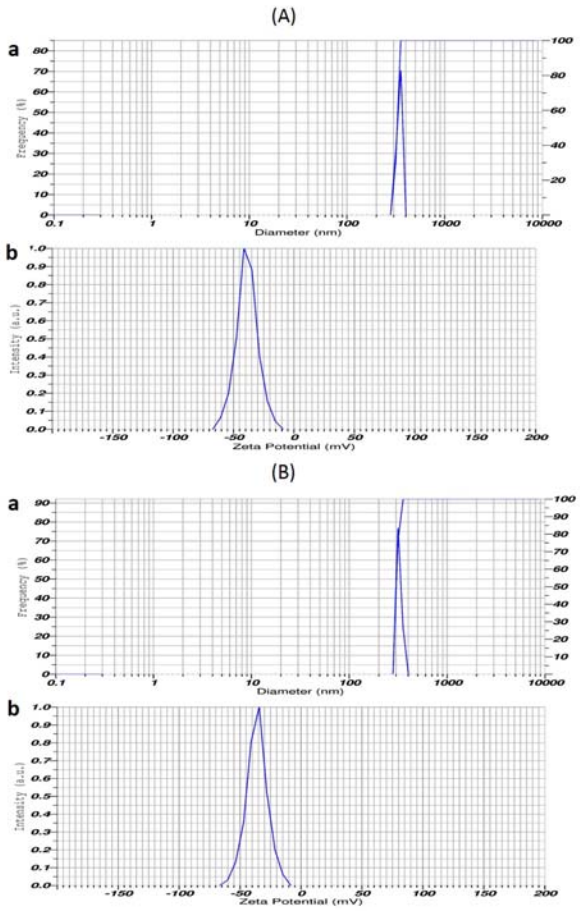

Figure 1 Particle size distribution (a) and zeta potential profiles (b) of ritonavir:Eudragit® L100-55 (A) and ritonavir:Kolliphor® P188 (B) solid dispersions.

Zeta potential, a commonly measured property of solid-dispersions, correlates to the surface interactions and points to the physical stability of micro- or nano-particulate formulations. The zeta potential of the optimized RE was -36.2 ± 2.3 mV (Figure 1Ab) and that of the optimized RP (Figure 1Bb) was -38.8 ± 1.9 mV. These observed values are indicative of an acceptable physical stability of the prepared solid dispersions, and similar to those reported earlier (27).

Photomicroscopy

Figure 2 (A, B, and C) shows the micro-scopically observed dimensional characteristics of ritonavir particles and the SD formulations. The figure compares the surface architecture of ritonavir (Figure 2A) with that of RE (Figure 2B) and RP (Figure 2C) at 20x magnification. The small, needle shaped crystalline particles of ritonavir (Figure 2A), corresponding to the polymorphic form III of ritonavir have been reported earlier (28). A dramatically different morphology was observed with both, RE and RP solid-dispersions. RE appeared transparent, large, sharp-edged, flat particles with a rough surface: whereas RP appeared relatively irregularly shaped, smooth/rounded-edged particles. The needle-shaped crystals of pure ritonavir were absent in images of RE and RP. These observations supported the formation of solid-dispersions.

Thermal analysis

The analysis of any drug-drug, drug-excipient, and/or excipient-excipient interactions in a formulation are often carried out using thermal techniques. Figure 3A compares the DSC profiles of (a) pure ritonavir, (b) pure Eudragit® L100-55, (c) the physical mixture (PM, 1:1) of ritonavir and Eudragit® L100-55, and (d) the solid dispersion of ritonavir with Eudragit® L100-55 (RE). As shown in Figure 3Aa, the DSC curve of pure ritonavir revealed a single, sharp endothermic peak around ~125ºC (melting point of ritonavir). Similar observations have been reported earlier (28). The thermogram of Eudragit® L100-55 (Figure 3Ab) was devoid of any significant event. However, a broad endothermic event, observed at around ~170-175°C, is most likely indicative of the beginning of the decomposition of Eudragit® L100-55 (29). The DSC profile of the PM (Figure 3Ac) exhibited a pattern of weak

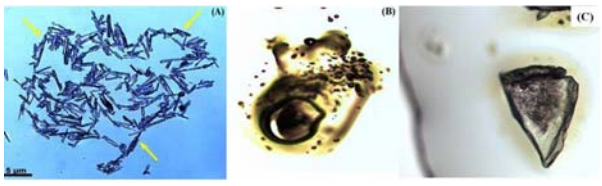

Figure 2 Photomicroscopy images of (A) pure ritonavir, (B) ritonavir:Eudragit® L100-55 solid dispersion, and (C) ritonavir:Kolliphor® P188 solid dispersions.

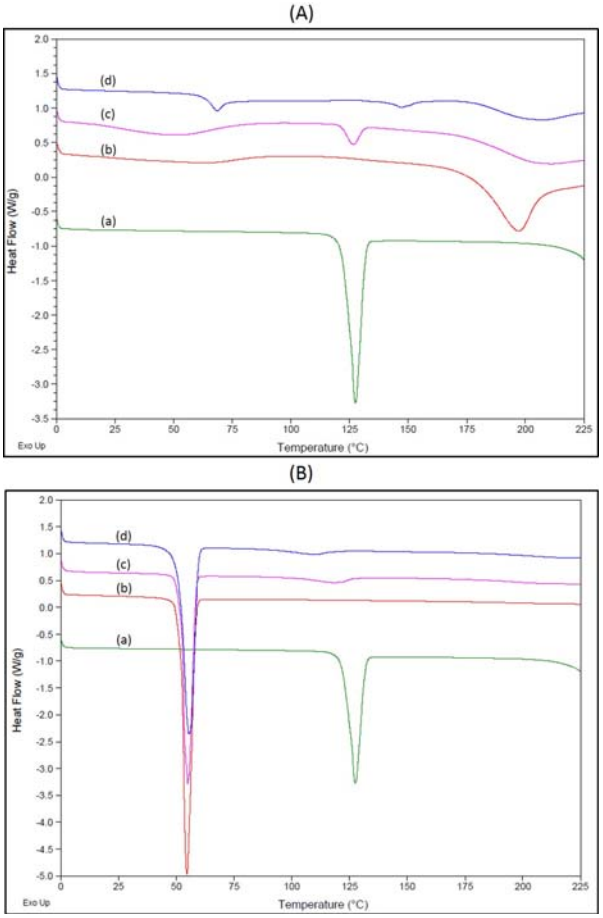

Figure 3 (A) Comparison of the DSC thermograms of (a) pure ritonavir, (b) pure Eudragit® L100-55, (c) the physical mixture (PM) of ritonavir and Eudragit® L100-55, and (d) the solid dispersion of ritonavir with Eudragit® L100-55 (RE). (B) Comparison of the DSC thermograms of (a) pure ritonavir, (b) pure Kolliphor® P188, (c) the physical mixture (PM) of ritonavir and Kolliphor® P188, and (d) the solid dispersion of ritonavir with Kolliphor® P188 (RP).

endothermic peaks that can be associated with both, ritonavir and Eudragit® L100-55. The melting peak of ritonavir in the mixture was weaker than that observed with pure ritonavir. The lower quantitative ratio of ritonavir in the mixture, as well as possible *in situ* interactions between ritonavir and Eudragit® L100-55 were likely contributors to these observations. Figure 3Ad shows the thermogram of the prepared solid dispersion of ritonavir with Eudragit® L100-55 (RE). This thermogram revealed very weak and undefined peak at ~70°C. This peak differed in the location of the temperature scale from the peaks obtained with pure ritonavir, Eudragit® L100-55, or their physical mixture, suggesting possible interactions between ritonavir and Eudragit® L100-55, resulting in the formation of an amorphous aggregate. Moreover, the sharp melting peak of ritonavir was absent in the thermogram of RE, thus supporting the possible amorphization of ritonavir (1).

Figure 3B compares the DSC profiles of (a) pure ritonavir, (b) pure Kolliphor® P188, (c) the physical mixture (PM, 1:1) of ritonavir and Kolliphor® P188, and (d) the solid dispersion of ritonavir with Kolliphor® P188 (RP). The thermogram of pure ritonavir (Figure 3Ba) was similar to the one observed before, with a single, sharp melting endotherm (~125°C) characteristic of crystalline material. The thermogram of Kolliphor® P188 (Figure 3Bb) also showed a single, sharp endotherm approximately between 50-55°C. This peak is characteristic of poloxamer melting point, and consistent with previously reported observations (30). The thermogram of PM (Figure 3Bc) revealed the poloxamer melting peak between 50-55°C. The ritonavir melting peak (125°C) was absent in this thermogram. Only an insignificant remnant, in the form of a broad, undefined, endothermic curve was observed between ~110-125°C. This disappearance of ritonavir melting peak can be attributed to the *in situ* molecular dispersion of ritonavir into the molten Kolliphor® P188. The thermogram of ritonavir-Kolliphor® P188 solid dispersion (RP) (Figure 3Bd) showed, as expected, a single, sharp endothermic peak representing Kolliphor® P188 melting; whereas the melting peak of ritonavir was absent. These observations support a successful formation of molecular aggregates of ritonavir and Kolliphor® P188 in the prepared solid dispersion.

Fourier transform infrared (FTIR) analysis

Figure 4 shows the FTIR spectra of (A) pure ritonavir, (B) Eudragit® L100-55, (C) PM, and (D) the solid dispersion of ritonavir with Eudragit® L100-55 (RE), respectively. The

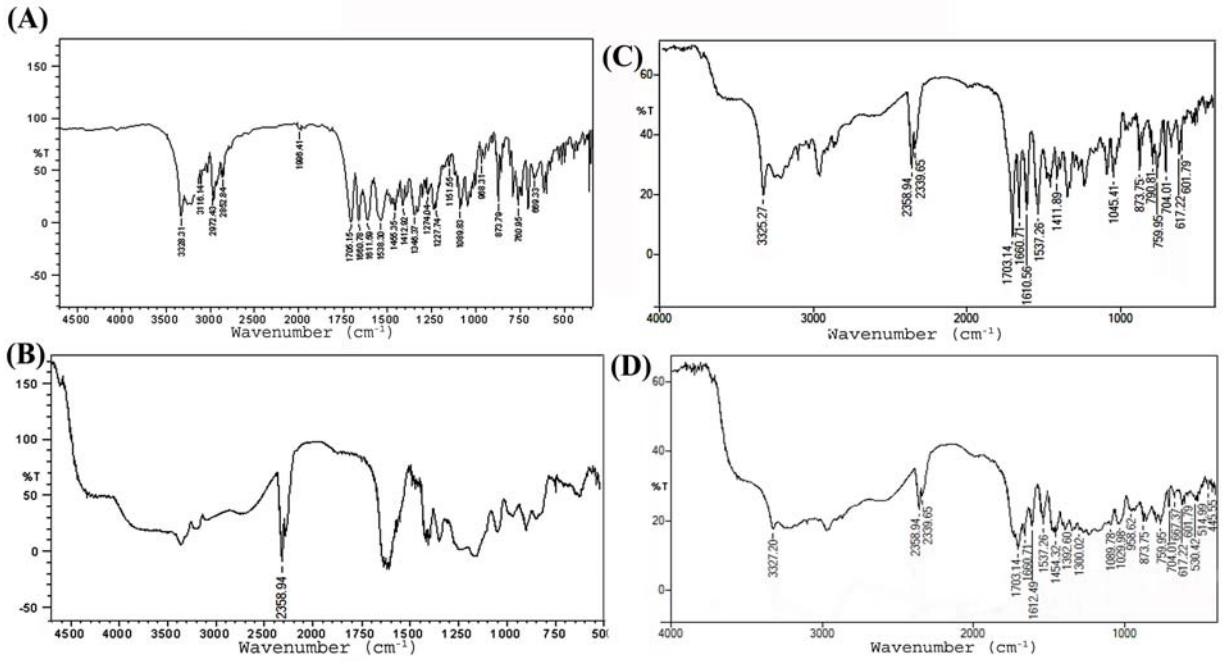

Figure 4 FTIR spectra of (A) pure ritonavir, (B) Eudragit® L100-55, (C) PM, and (D) the solid dispersion of ritonavir with Eudragit® L100-55 (RE).

spectrum of pure ritonavir (Figure 4A) exhibited molecule-specific peaks similar to those reported earlier (7). The FTIR spectrum of Eudragit® L100-55 is shown in the Figure 4B. This spectrum revealed a broader band, characteristic of a hydroxyl group (O-H stretch vibration) at 2358 cm^{-1}, a strong peak related to the carbonyl group (C-O stretch vibration) at 1733 cm^{-1}, and two bands at 1368 cm^{-1} and 1266 cm^{-1} related to ester linkages (C-O stretch vibration). The spectrum of PM (Figure 4C) showed peaks characteristic of both the individual components of the mixture i.e., pure ritonavir and Eudragit® L100-55. Figure 4D shows the FTIR spectrum of the prepared solid dispersion of ritonavir with Eudragit® L100-55 (RE). This spectrum was devoid of the key peaks *viz.* 3116 cm^{-1}, 2972 cm^{-1} and 2852 cm^{-1}, associated with ritonavir. The absence of ritonavir peaks in the FTIR spectrum of the prepared solid dispersion indicated the interaction of ritonavir with Eudragit® L100-55 at a molecular level. The ritonavir molecules likely dispersed within Eudragit® L100-55 matrix.

Figure 5 compares the FTIR spectra of (A) pure ritonavir, (B) pure Kolliphor® P188, (C) the physical mixture (PM) of ritonavir and Kolliphor® P188, and (D) the solid dispersion of ritonavir with Kolliphor® P188 (RP). The spectrum of pure ritonavir (Figure 5A) revealed all the characteristic peaks of ritonavir described above. The spectrum of Kolliphor® P188 (Figure 5B) exhibited absorption peaks at 2886 cm^{-1} and 1546 cm^{-1} related to O-H and C-O stretching, respectively. This spectrum also showed additional peaks at 1467 cm^{-1}, 1359 cm^{-1}, 1278 cm^{-1}, 954 cm^{-1}, and 842 cm^{-1}. Figure 5C shows the spectrum of the physical mixture (PM). This spectrum revealed that all the peaks associated with ritonavir and Kolliphor® P188 were retained, indicating a lack of any interaction between the components. The spectrum of the ritonavir-Kolliphor® P188 solid dispersion (Figure 5D) was devoid of the characteristic peaks associated with either component. Moreover, two additional peaks were observed at 3502 cm^{-1} and 2880 cm^{-1}, in this spectrum. Hydrogen bonding between the

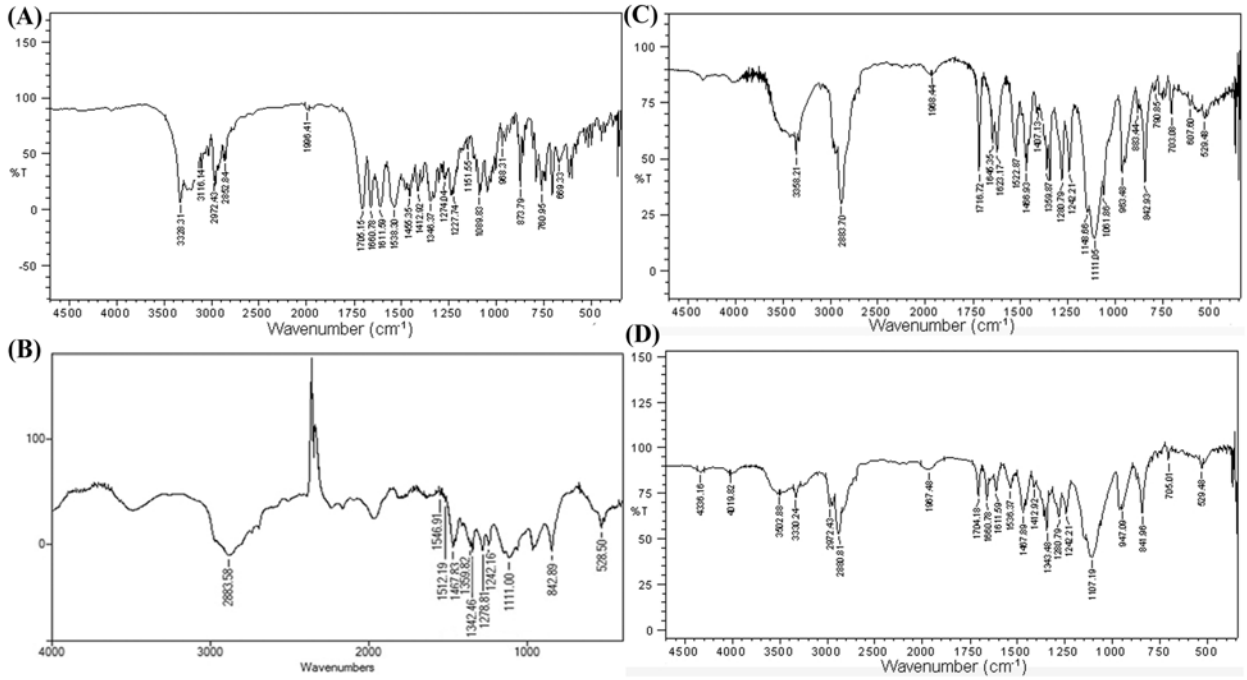

Figure 5 FTIR spectra of (A) pure ritonavir, (B) Kolliphor® P188, (C) PM, and (D) the solid dispersion of ritonavir with Kolliphor® P188 (RP).

components of solid dispersion may have resulted in the appearance of these peaks. These observations support our inference of molecular dispersion of ritonavir within Kolliphor® P188 matrix.

X-ray diffractometry

The solid-state properties of the prepared solid dispersions (RE and RP), compared with pure ritonavir, were further examined using powder x-ray diffractometry (PXRD). Figure 6 shows the x-ray diffractograms of (A) pure ritonavir, (B) the solid dispersion of ritonavir with Eudragit® L100-55 (RE), and (C) the solid dispersion of ritonavir with Kolliphor® P188 (RP). The diffractograms are plotted in the form of intensity (counts) on a 2θ scale. The diffractogram of pure ritonavir (Figure 6A) revealed several sharp peaks, characteristic of its crystalline nature, in the region of 5-50° 2θ. These observations are in agreement with those reported earlier in the literature (7, 28). Figure 6B shows the diffractogram of the prepared solid-dispersion of ritonavir with Eudragit® L100-55 (RE). This diffractogram exhibited a single, broad, and undefined peak (halo), typically associated with amorphous materials. Most of the characteristic crystalline peaks of ritonavir were absent. Similarly, in the diffractogram of the solid dispersion of ritonavir with Kolliphor® P188 (RP) (Figure 6C) was devoid of most of the crystalline peaks of ritonavir. Only two peaks *viz.* at 19 2θ and 23 2θ, which can be attributed to ritonavir were observed. These observations led us to infer that in the ritonavir- Kolliphor® P188 (RP), ritonavir is at least partially amorphized. Overall, these results support a reduction in ritonavir crystallinity, and its partial amorphization.

Performance evaluation of the ritonavir dispersions

Ritonavir dissolution

Figure 7 compares the dissolution profiles (ritonavir release, %) of pure ritonavir, with that of the prepared solid dispersions of ritonavir, with different ratios of Eudragit® L100-55 (Figure 7A, RE-1 to RE-4) or Kolliphor® P188

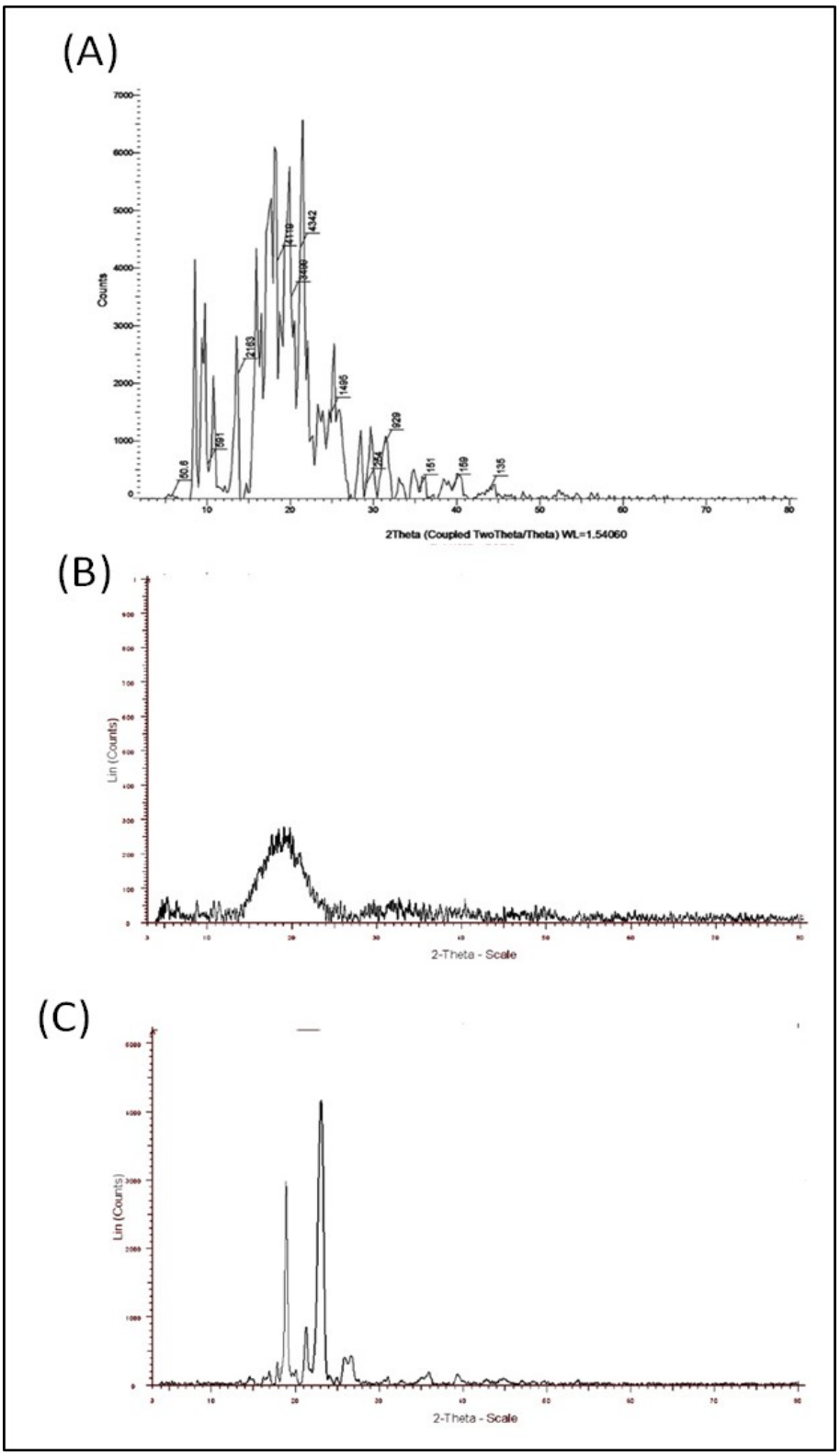

Figure 6 X-ray diffractograms of (A) pure ritonavir, (B) the solid dispersion of ritonavir with Eudragit® L100-55 (RE), and (C) the solid dispersion of ritonavir with Kolliphor® P188 (RP).

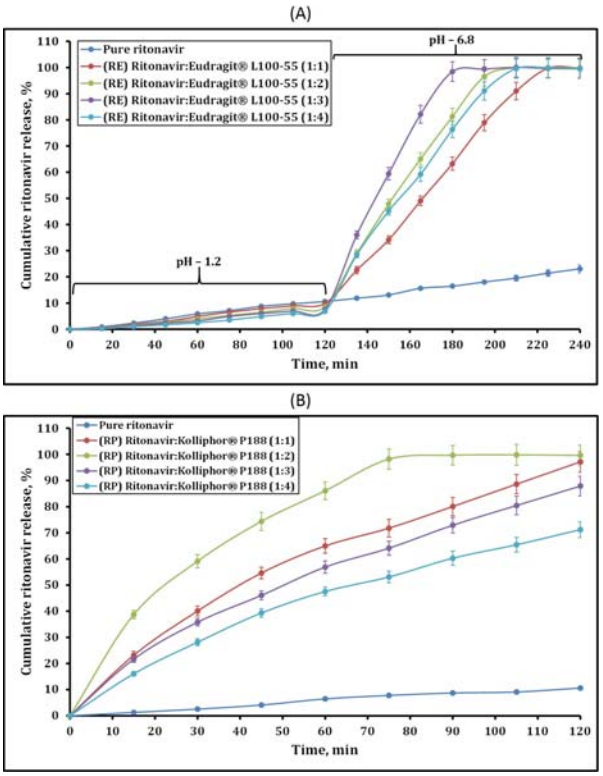

Figure 7 *In vitro* dissolution profiles of pure ritonavir and the solid dispersions of ritonavir with different ratios of (A) Eudragit® L100-55 or (B) Kolliphor® P188.

(Figure 7B, RP-1 to RP-4). The dissolution of RE formulations was carried out in HCl (0.1N, pH-1.2) for the first two hours, followed by phosphate buffer (0.05M, pH-6.8) for an additional two hours. The dissolution of RP formulations was carried out in phosphate buffer (0.05M, pH-6.8) for four hours. As shown in Figure 7A, pure ritonavir exhibited ~23% dissolution at the end of 6 h evaluation period. Considering the practically insoluble nature of the molecule, these observations are expected, and consistent with the results reported earlier. For the ritonavir: Eudragit® L100-55 solid dispersions, the rate and extent of ritonavir release followed a similar path to that of pure ritonavir for the first two hours (in acidic conditions). Thereafter, the rate and extent of ritonavir release from the solid dispersions were observed to progressively increase with increasing ratio of Eudragit® L100-55 in the formulation, up to the ritonavir: carrier ratio of 1:3. For the formulation with ritonavir:Eudragit® L100-55 ratio of 1:4, the rate and extent of ritonavir dissolution was found to be lower, and similar to the formulation with the ritonavir: carrier ratio of 1:2. These observations correlated well with the results obtained from the saturation solubility studies (Table 1), i.e. aqueous solubility of ritonavir appeared to increase with increasing ratio of Eudragit® L100-55, up to the ritonavir:carrier ratio of 1:3 and lower for ritonavir:Eudragit® L100-55 ratio of 1:4. The formulation containing ritonavir:Eudragit® L100-55 ratio of 1:3 demonstrated a near 100% release of ritonavir within three hours of dissolution. This ratio, thus appeared to be an optimal ratio in regards to enhancing ritonavir solubility and dissolution. Overall, these solid dispersions exhibited greater extent of ritonavir release compared to the native solubility of the pure ritonavir, possibly due to decreased crystallinity of ritonavir within the polymer matrix, and likely formation of a supersaturated liquid state in the dissolution medium (31). A reduction in enthalpy of the system is typically associated with the observed improvement in the dissolution rates of amorphous solid dispersions, compared to that of crystalline materials (32, 33). All the RE formulations sustained the ritonavir release since Eudragit® L100-55 is characterized for maintaining supersaturation (34-36).

Figure 7B shows the comparative dissolution performance of pure ritonavir and the prepared solid dispersions of ritonavir with different ratios of Kolliphor® P1188 in phosphate buffer (pH-6.8). At the end of the evaluation period, pure ritonavir exhibited only ~11% dissolution in the phosphate buffer. Similar to the ritonavir: Eudragit® L100-55 solid dispersions, the rate and extent of ritonavir release from these dispersions was observed to increase with increasing amounts of Kolliphor® P1188, upto a ritonavir:carrier ratio of 1:2. Further increases in the Kolliphor® P188 ratio appeared to decrease the rate and extent of ritonavir release from these formulations. These observations

mirrored those from the saturation solubility studies (Table 1), where aqueous solubility of ritonavir was found to be highest in the formulation with ritonavir:Kolliphor® P1188 ratio of 1:2. Ritonavir:Kolliphor® P188 formulation with a ratio of 1:2 showed ~100% ritonavir release within 90 min dissolution. This formulation was thus found to be optimal considering the goal of improving the solubility/dissolution of ritonavir. The lyophilization-induced formation of porous particles with high surface area, and subsequently increased surface energies, could have contributed to the overall increase in ritonavir solubility/dissolution exhibited by these solid dispersions. (22, 37). Finally, the hydrophobic polyoxypropylene center block in poloxamers assist them in adsorbing strongly onto the surface of hydrophobic particles (38). The hydrophilic polyoxyethylene side-chain thus extends outward from the particle surface, and stabilizes the particle suspension (39, 40). The observed decrease in the rate and extent of ritonavir release at higher Kolliphor® P188 ratios could be attributed to its gel forming property, resulting in a larger diffusion barrier for ritonavir (3).

Dissolution efficiency (DE)

Table 2 shows a comparison of the dissolution efficiencies (DE) of pure ritonavir with that of the prepared dispersions of ritonavir with different ratios of Eudragit® L100-55 (RE-1 to RE-4) or Kolliphor® P188 (RP-1 to RP-4) carried out in [0.1N HCl/phosphate buffer, pH-6.8] or phosphate buffer (pH-6.8), respectively. Depending on the dissolution media employed, the DE values of pure ritonavir were observed to be ~11% or ~5.7%. Consistent with the dissolution study results, and as expected, the DE values for the ritonavir: Eudragit® L100-55 solid dispersions progressively increased with increasing ratio of Eudragit® L100-55 in the formulation, up to the ritonavir:carrier ratio of 1:3. For the formulation with ritonavir:Eudragit® L100-55 ratio of 1:4, the DE value was found to be lower, and closer to the formulation with the ritonavir:carrier ratio of 1:2. The formulation containing ritonavir:Eudragit® L100-55 ratio of 1:3 demonstrated a significant increase in the DE value (~41 %, > 3.5-times) compared to pure ritonavir. Similarly, the DE values of the solid dispersions was observed to increase with increasing amounts of Kolliphor® P1188, up to the ritonavir: carrier ratio of 1:2. Further increases in the Kolliphor® P188 ratio appeared to decrease the DE values of these formulations. Dispersions containing ritonavir: Kolliphor® P188 in the ratio of 1:2 demonstrated a significant increase in the DE value (~75%, > 13-times) compared to pure ritonavir. The increased aqueous solubility of ritonavir in the prepared solid dispersions is likely a major contributor for the observed increase in DE. A decrease in DE observed with higher polymer ratio in the solid dispersions can be attributed to the causes mentioned above.

Table 2 Dissolution efficiency of ritonavir in the prepared solid dispersions

DRUG: CARRIER RATIO	DISSOLUTION EFFICIENCY	
	RITONAVIR:EUDRAGIT® L 100-55	RITONAVIR:KOLLIPHOR® P188
Pure Ritonavir	10.95 ± 0.37	5.68 ± 0.23
1:1	33.19 ± 0.89	58.87 ± 1.13
1:2	37.83 ± 0.53	75.17 ± 1.42
1:3	40.75 ± 1.03	52.76 ± 0.95
1:4	35.94 ± 0.97	43.29 ± 0.83

*Values represent mean ± Std. Dev. (n=3)

Fasted versus fed state dissolution

Figure 8 shows the dissolution results for the optimized dispersions of ritonavir with Eudragit® L100-55 or Kolliphor® P188 carried out in biorelevant media *viz.* FaSSIF (Figure 8A) or FeSSIF (Figure 8B) to assess the influence of food on the release of ritonavir. Pure ritonavir showed a significantly slower dissolution in the FaSSIF media, with ~14% released at the end of two-hour dissolution period. However, in the FeSSIF (fed) media, the rate and extent of ritonavir was ~32% (~2-

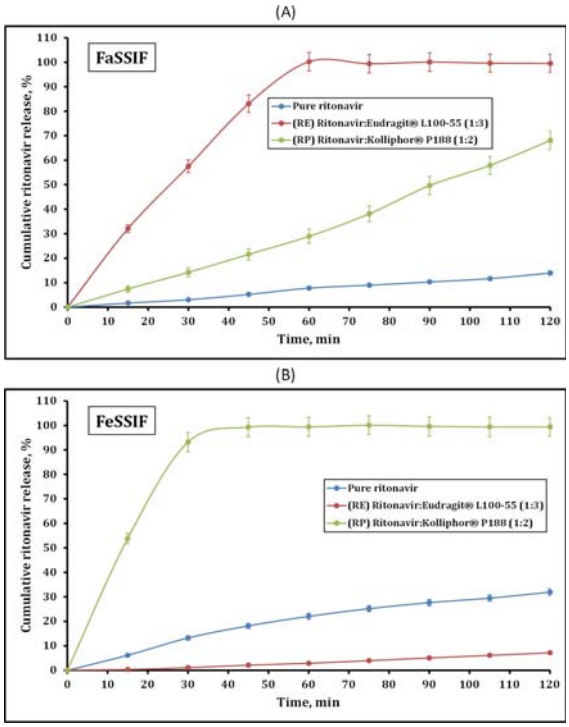

Figure 8 *In vitro* dissolution profiles of the optimized solid dispersions of ritonavir with Eudragit® L100-55 or Kolliphor® P188 in (A) FaSSIF medium and (B) FeSSIF medium.

fold increase) at the end of testing period. These results are consistent with previously reported observations regarding the positive influence of food on the oral absorption of ritonavir (41).

In the FaSSIF media, the optimized solid dispersions of ritonavir with Eudragit® L100-55 (RE) showed a significant increase in the rate and extent of ritonavir release. Nearly 100% of ritonavir were released within an hour of testing period. These observations were expected considering the pH of the FaSSIF media and the pH-dependent characteristics of the polymer. The optimized dispersions of ritonavir with Kolliphor® P188 exhibited a near-linear, and a significantly higher rate and extent of ritonavir release, with ~70 % ritonavir released at the end of the evaluation period. In the FeSSIF media, the optimized solid dispersions of ritonavir with Eudragit® L100-55 (RE) showed a significantly lower rate and extent of ritonavir release. Only about 7% ritonavir was observed to be released in the 120 minute evaluation period. Eudragit® L100-55, being a pH-dependent enteric polymer, and the acidic environment of the FeSSIF media may have contributed to the slower release of ritonavir. The optimized dispersions of ritonavir with Kolliphor® P188 exhibited a significantly faster rate and extent of ritonavir release in the FeSSIF media. Nearly 100% of ritonavir was observed to be released within the first 45 minutes of the dissolution period. These results demonstrate the importance of selecting a carrier polymer for formulating solid dispersions. In the current study, the performance of ritonavir solid dispersion containing Kolliphor® P188 appears to be least influenced by the presence/absence of food.

Ritonavir permeability

Figure 9 shows ritonavir permeability from the prepared dispersions of ritonavir with different amounts of Eudragit® L100-55 (Figure 9A, RE-1 to RE-4) or Kolliphor® P188 (Figure 9B, RP-1 to RP-4) as compared to that of pure ritonavir. Overall, the permeability profiles of these solid dispersions followed a pattern similar to that observed within the *in vitro* dissolution studies.

Figure 9A shows the *ex vivo* permeability profiles of the prepared solid dispersions of ritonavir with different ratios of Eudragit® L100-55 (RE-1 to RE-4). Pure ritonavir exhibited poor permeability across the intestinal membrane, with only ~20% traversed at the end of the 180 minute evaluation period. For the ritonavir:Eudragit® L100-55 solid dispersions, the rate and extent of ritonavir permeation was observed to progressively increase with increasing amount of Eudragit® L100-55 in the formulation, up to the ritonavir:carrier ratio of 1:3. For the formulation with ritonavir:Eudragit® L100-55 ratio of 1:4, the rate and extent of ritonavir permeation was found to be lower, and similar to the formulation with the ritonavir:carrier

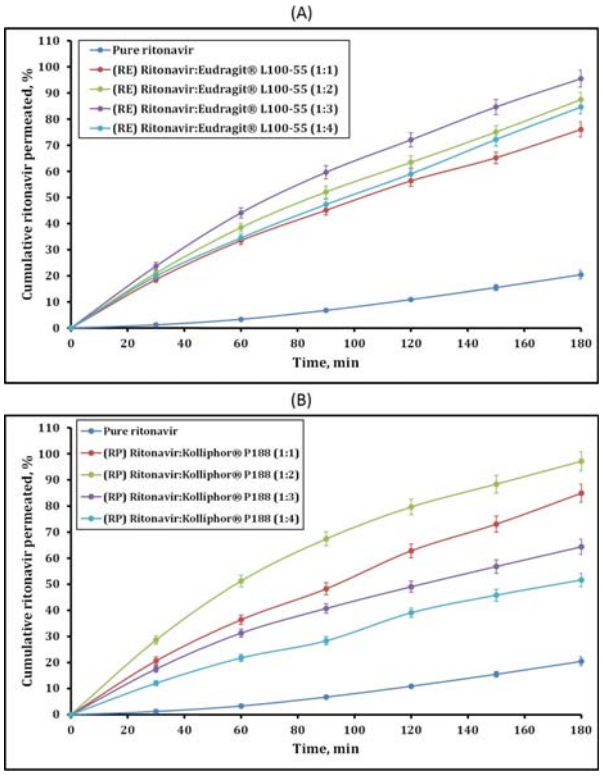

Figure 9 *Ex vivo* permeability profiles of the solid dispersions of ritonavir with different ratios of (A) Eudragit® L100-55 and (B) Kolliphor® P188, when compared to pure ritonavir.

ratio of 1:2. The formulation containing ritonavir:Eudragit® L100-55 ratio of 1:3 demonstrated ~95% of ritonavir permeation at the end of 180 min evaluation period. For ritonavir: Kolliphor® P188 solid dispersions (Figure 9B), the rate and extent of ritonavir permeation was observed to increase with increasing amounts of Kolliphor® P188, up to the ritonavir: carrier ratio of 1:2. Further increases in the Kolliphor® P188 ratio appeared to lower the rate and extent of ritonavir permeation from these formulations. Ritonavir:Kolliphor® P188 formulation with a ratio of 1:2 showed ~97% ritonavir permeation at the end of 3 hours. Within the class of HIV-1 protease inhibitors, ritonavir has the lowest partition coefficient (3.9) (42). The overall higher permeability of ritonavir observed with the prepared solid dispersions could be attributed to the amphiphilic nature of the carriers. Kolliphor® P188, besides being surfactant and co-emulsifier, is known to be an inhibitor of P-gp and CYP3A4. This property of Kolliphor® P188 might have contributed to a decrease in efflux of ritonavir from intestinal cells, and resulted in enhancement of ritonavir transport across the intestinal segment (43).

Preliminary functional stability assessment

The final solid dispersions, i.e. ritonavir:Eudragit® L100-55 (1:3, RE-3) and ritonavir:Kolliphor® P188 (1:2, RP-2) were assessed for a six-month stability 25 °C at 60 % RH. These formulations were then assessed for the dissolution and permeability of ritonavir. These attributes were then compared to the results obtained prior to storage. Figure 10A shows a comparison of the dissolution performance of ritonavir:Eudragit® L100-55 solid dispersion subjected to controlled conditions for six months with that at day 0.

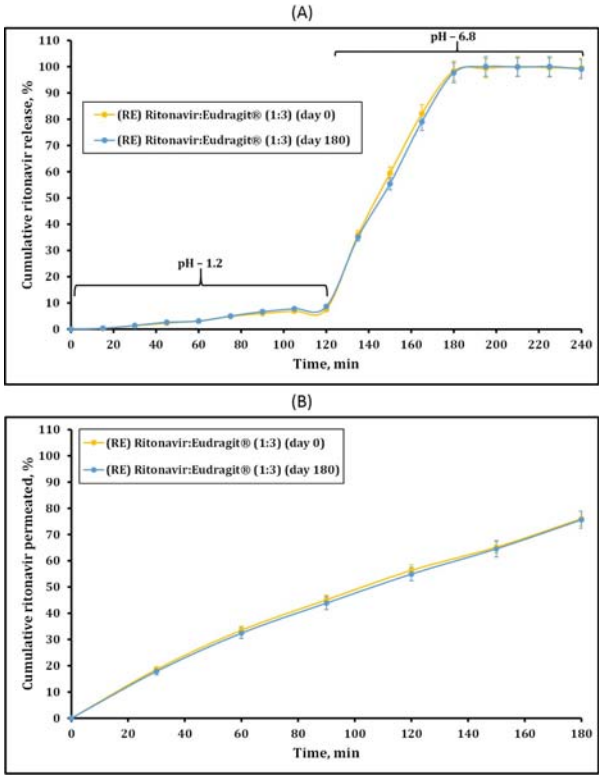

Figure 10 Comparison of the (A) *in vitro* dissolution and (B) *ex-vivo* permeability of the optimized solid dispersions of ritonavir with Eudragit® L100-55, before and after six months of storage at 25°C/60% RH.

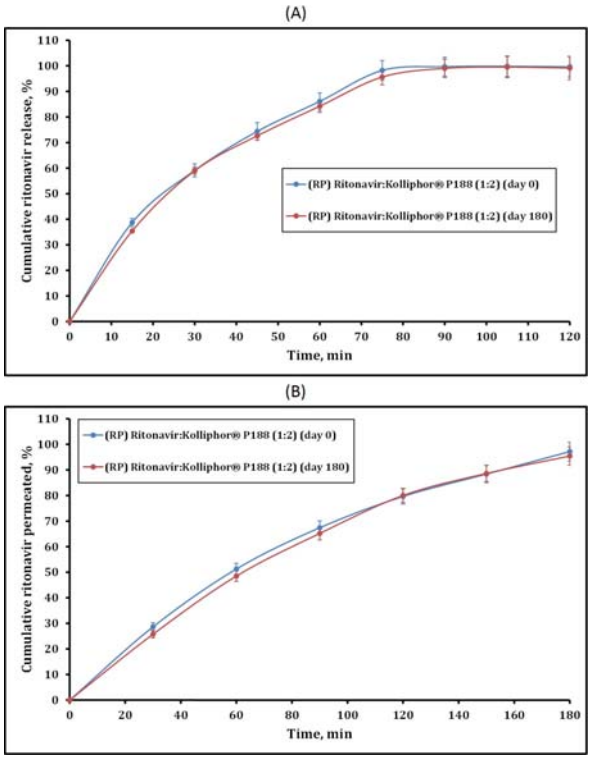

Figure 11 Comparison of the (A) *in vitro* dissolution and (B) *ex-vivo* permeability of the optimized solid dispersions of ritonavir with Kolliphor® P188, before and after six month storage at 25°C at 60% RH.

The rate and extent of dissolution for both samples were similar, and no significant differences were observed in their profiles. Similarly, a comparison of the ritonavir permeability (Figure 10B) from these samples showed that the rate and extent of ritonavir permeation were not influenced by storage conditions. These results indicate the relative robustness of the optimized ritonavir: Eudragit® L100-55 solid dispersion that is functionally stable.

The dissolution performance of the ritonavir: Kolliphor® P188 solid dispersion stored for six months at 25°C/60% RH was similar to that of the initial solid-dispersion formulation (Figure 11A). At the end of the 120 minute evaluation period, the sample subjected to 180-day stability was found to release nearly 100% of ritonavir, similar to the formulation on day 0. No significant difference was found between the dissolution performances of both samples. The results of the comparison of ritonavir permeability from ritonavir:Kolliphor® P188 solid dispersion stored at controlled conditions for 180 days with that of initial samples are shown in Figure 11B. The ritonavir permeability performance of both samples were similar, without any significant differences in the rate and extent of ritonavir permeability between the samples. While these results indicate potentially robust and relatively stable formulation, additional stability studies are warranted to examine any physico-chemical changes resulting in the formulations upon storage. Such studies can also shed light on the potential recrystallization of the ritonavir in the solid dispersions upon prolonged storage.

CONCLUSIONS

The present work explored the feasibility of optimizing the amounts of a carrier (Eudragit® L100-55 or Kolliphor® P188) used to prepare solid dispersions of ritonavir, while increasing its solubility, dissolution, and permeability. The prepared solid dispersions were optimized to achieve maximum functionality at the lowest carrier-polymer incorporation level. The analysis of prepared solid dispersions via photomicroscopy, particle size analysis, thermal analysis, FTIR, and PXRD supported the formation of dispersions. The solubility of ritonavir increased significantly when it was formulated into a solid dispersion. The results from the dissolution and permeation studies revealed a significant improvement in ritonavir release and permeability from these dispersions, compared to pure ritonavir. A preliminary stability assessment study demonstrated the functional stability of prepared solid dispersions. A solid dispersion approach can be successfully implemented to improve the solubility and permeability of drugs with poor aqueous solubility *via* careful selection of carrier polymers and optimization of formulation variables.

ACKNOWLEDGEMENTS

The authors are thankful to the Science and Engineering Research Board (Department of Science and Technology), Government of India for the financial assistance to this research project (SB/YS/LS-291/2013).

REFERENCES

1 Vo CL-N, Park C, Lee B-J. Current trends and future perspectives of solid dispersions containing poorly water-soluble drugs. Eur J Pharm Biopharm. 2013;85(3, Part B):799-813. doi: http://dx.doi.org/10.1016/j.ejpb.2013.09.007.

2 Kawabata Y, Wada K, Nakatani M, Yamada S, Onoue S. Formulation design for poorly water-soluble drugs based on biopharmaceutics classification system: Basic approaches and practical applications. Int J Pharm. 2011;420(1):1-10. doi: http://dx.doi.org/10.1016/j.ijpharm.2011.08.032.

3 Van den Mooter G. The use of amorphous solid dispersions: A formulation strategy to overcome poor solubility and dissolution rate. Drug Discovery Today: Technologies. 2012;9(2):e79-e85. doi: http://dx.doi.org/10.1016/j.ddtec.2011.10.002.

4 Zhang M, Li H, Lang B, O'Donnell K, Zhang H, Wang Z, et al. Formulation and delivery of improved amorphous fenofibrate solid dispersions prepared by thin film freezing. Eur J Pharm Biopharm. 2012;82(3):534-44. doi: 10.1016/j.ejpb.2012.06.016.

5 Chiou WL, Riegelman S. Pharmaceutical applications of solid dispersion systems. J Pharm Sci. 1971;60(9):1281-302. doi: 10.1002/jps.2600600902.

6 Lea AP, Faulds D. Ritonavir. Drugs. 1996;52(4):541-6. doi: 10.2165/00003495-199652040-00007.

7 Dhore PW, Dave VS, Saoji SD, Bobde YS, Mack C, Raut NA. Enhancement of the aqueous solubility and permeability of a poorly water soluble drug ritonavir via lyophilized milk-based solid dispersions. Pharm Dev Technol. 2016:1-13. doi: 10.1080/10837450.2016.1193193.

8 Law D, Krill SL, Schmitt EA, Fort JJ, Qiu Y, Wang W, et al. Physicochemical considerations in the preparation of amorphous ritonavir-poly(ethylene glycol) 8000 solid dispersions. J Pharm Sci. 2001;90(8):1015-25.

9 Law D, Schmitt EA, Marsh KC, Everitt EA, Wang W, Fort JJ, et al. Ritonavir-PEG 8000 amorphous solid dispersions: in vitro and in vivo evaluations. J Pharm Sci. 2004;93(3):563-70. doi: 10.1002/jps.10566.

10 WebMD. List ritonavir side effects by likelihood and severity. USA: WebMD; 2017 [cited 2017 2/19/2017]; Available from: http://www.webmd.com/drugs/2/drug-8436-1138/ritonavir-oral/ritonavir---oral/details/list-sideeffects.

11 Lee RC, River LP, Pan FS, Ji L, Wollmann RL. Surfactant-induced sealing of electropermeabilized skeletal muscle membranes in vivo. Proc Natl Acad Sci U S A. 1992;89(10):4524-8.

12 Moloughney JG, Weisleder N. Poloxamer 188 (p188) as a membrane resealing reagent in biomedical applications. Recent Pat Biotechnol. 2012;6(3):200-11.

13 Tran T-H, Park C, Kang T, Park Y-J, Oh E, Lee B-J. Micromeritic properties and instrumental analysis of physical mixtures and solid dispersions with adsorbent containing losartan: Comparison of dissolution-differentiating factors. Powder Technol. 2015;272:269-75. doi: http://dx.doi.org/10.1016/j.powtec.2014.12.007.

14 Sonar PA, Behera AL, Banerjee SK, Gaikwad DD, Harer SL. Preparation and characterization of Simvastatin solid dispersion using skimmed milk. Drug Dev Ind Pharm. 2015;41(1):22-7. doi: 10.3109/03639045.2013.845836.

15 Sze A, Erickson D, Ren L, Li D. Zeta-potential measurement using the Smoluchowski equation and the slope of the current–time relationship in electroosmotic flow. J Colloid Interface Sci. 2003;261(2):402-10. doi: http://dx.doi.org/10.1016/S0021-9797(03)00142-5.

16 Saoji SD, Belgamwar VS, Dharashivkar SS, Rode AA, Mack C, Dave VS. The Study of the Influence of Formulation and Process Variables on the Functional Attributes of Simvastatin–Phospholipid Complex. J Pharm Innov. 2016;11(3):264-78. doi: 10.1007/s12247-016-9256-7.

17 Saoji SD, Atram SC, Dhore PW, Deole PS, Raut NA, Dave VS. Influence of the Component Excipients on the Quality and Functionality of a Transdermal Film Formulation. AAPS PharmSciTech. 2015;16(6):1344-56. doi: 10.1208/s12249-015-0322-0.

18 Anderson NH, Bauer M, Boussac N, Khan-Malek R, Munden P, Sardaro M. An evaluation of fit factors and dissolution efficiency for the comparison of in vitro dissolution profiles. J Pharm Biomed Anal. 1998;17(4–5):811-22. doi: http://dx.doi.org/10.1016/S0731-7085(98)00011-9.

19 Klein S. The Use of Biorelevant Dissolution Media to Forecast the In Vivo Performance of a Drug. The AAPS Journal. 2010;12(3):397-406. doi: 10.1208/s12248-010-9203-3.

20 Saoji SD, Raut NA, Dhore PW, Borkar CD, Popielarczyk M, Dave VS. Preparation and Evaluation of Phospholipid-Based Complex of Standardized Centella Extract (SCE) for the Enhanced Delivery of Phytoconstituents. AAPS J. 2016;18(1):102-14. doi: 10.1208/s12248-015-9837-2.

21 Bouma M, Nuijen B, Sava G, Perbellini A, Flaibani A, van Steenbergen MJ, et al. Pharmaceutical development of a parenteral lyophilized formulation of the antimetastatic ruthenium complex NAMI-A. Int J Pharm. 2002;248(1-2):247-59.

22 Patel BB, Patel JK, Chakraborty S. Solubility enhancement using poly(meth)acrylate based solid dispersions. Powder Technol. 2015;270, Part A:27-38. doi: http://dx.doi.org/10.1016/j.powtec.2014.10.006.

23 Sudhakar B, Krishna MC, Murthy KVR. Factorial design studies of antiretroviral drug-loaded stealth liposomal injectable: PEGylation, lyophilization and pharmacokinetic studies. Applied Nanoscience. 2016;6(1):43-60. doi: 10.1007/s13204-015-0408-8.

24 Rarokar NR, Saoji SD, Raut NA, Taksande JB, Khedekar PB, Dave VS. Nanostructured Cubosomes in a Thermoresponsive Depot System: An Alternative Approach for the Controlled Delivery of Docetaxel. AAPS PharmSciTech. 2016;17(2):436-45. doi: 10.1208/s12249-015-0369-y.

25 LeFevre ME, Olivo R, Vanderhoff JW, Joel DD. Accumulation of latex in Peyer's patches and its subsequent appearance in villi and mesenteric lymph nodes. Proc Soc Exp Biol Med. 1978;159(2):298-302.

26 Savic R, Luo L, Eisenberg A, Maysinger D. Micellar nanocontainers distribute to defined cytoplasmic organelles. Science. 2003;300(5619):615-8. doi: 10.1126/science.1078192.

27 Freitas C, Müller RH. Effect of light and temperature on zeta potential and physical stability in solid lipid nanoparticle (SLN™) dispersions. Int J Pharm. 1998;168(2):221-9. doi: http://dx.doi.org/10.1016/S0378-5173(98)00092-1.

28 Morissette SL, Soukasene S, Levinson D, Cima MJ, Almarsson O. Elucidation of crystal form diversity of the HIV protease inhibitor ritonavir by high-throughput crystallization. Proc Natl Acad Sci U S A. 2003;100(5):2180-4. doi: 10.1073/pnas.0437744100.

29 Parikh T, Gupta SS, Meena A, Serajuddin ATM. Investigation of thermal and viscoelastic properties of polymers relevant to hot melt extrusion - III: Polymethacrylates and polymethacrylic acid based polymers. Journal of Excipients and Food Chemicals. 2014;5(1):56-64.

30 Moghimi SM, Hunter AC, Dadswell CM, Savay S, Alving CR, Szebeni J. Causative factors behind poloxamer 188 (Pluronic F68, Flocor™)-induced complement activation in human sera: A protective role against poloxamer-mediated complement activation by elevated serum lipoprotein levels. Biochimica et Biophysica Acta (BBA) - Molecular Basis of Disease. 2004;1689(2):103-13. doi: http://dx.doi.org/10.1016/j.bbadis.2004.02.005.

31 Zecevic DE, Meier R, Daniels R, Wagner K-G. Site specific solubility improvement using solid dispersions of HPMC-AS/HPC SSL – Mixtures. Eur J Pharm Biopharm. 2014;87(2):264-70. doi: http://dx.doi.org/10.1016/j.ejpb.2014.03.018.

32 DiNunzio JC, Brough C, Miller DA, Williams Iii RO, McGinity JW. Applications of KinetiSol® Dispersing for the production of plasticizer free amorphous solid dispersions. Eur J Pharm Sci. 2010;40(3):179-87. doi: http://dx.doi.org/10.1016/j.ejps.2010.03.002.

33 Hughey JR, DiNunzio JC, Bennett RC, Brough C, Miller DA, Ma H, et al. Dissolution enhancement of a drug exhibiting thermal and acidic decomposition characteristics by fusion processing: a comparative study of hot melt extrusion and KinetiSol dispersing. AAPS PharmSciTech. 2010;11(2):760-74. doi: 10.1208/s12249-010-9431-y.

34 Curatolo W, Nightingale JA, Herbig SM. Utility of hydroxypropylmethylcellulose acetate succinate (HPMCAS) for initiation and maintenance of drug supersaturation in the GI milieu. Pharm Res. 2009;26(6):1419-31. doi: 10.1007/s11095-009-9852-z.

35 Friesen DT, Shanker R, Crew M, Smithey DT, Curatolo WJ, Nightingale JAS. Hydroxypropyl Methylcellulose Acetate Succinate-Based Spray-Dried Dispersions: An Overview. Mol Pharm. 2008;5(6):1003-19. doi: 10.1021/mp8000793.

36 Miller DA, DiNunzio JC, Yang W, McGinity JW, Williams RO, 3rd. Enhanced in vivo absorption of itraconazole via stabilization of supersaturation following acidic-to-neutral pH transition. Drug Dev Ind Pharm. 2008;34(8):890-902. doi: 10.1080/03639040801929273.

37 Simonelli AP, Mehta SC, Higuchi WI. Dissolution Rates of High Energy Polyvinylpyrrolidone (PVP)-Sulfathiazole Coprecipitates. J Pharm Sci. 1969;58(5):538-49. doi: 10.1002/jps.2600580503.

38 Storm G, Belliot SO, Daemen T, Lasic DD. Surface modification of nanoparticles to oppose uptake by the mononuclear phagocyte system. Adv Drug Delivery Rev. 1995;17(1):31-48. doi: http://dx.doi.org/10.1016/0169-409X(95)00039-A.

39 Li J-T, Caldwell KD. Plasma protein interactions with Pluronic™-treated colloids. Colloids and Surfaces B: Biointerfaces. 1996;7(1–2):9-22. doi: http://dx.doi.org/10.1016/0927-7765(96)01269-6.

40 Moghimi SM, Muir IS, Illum L, Davis SS, Kolb-Bachofen V. Coating particles with a block co-

polymer (poloxamine-908) suppresses opsonization but permits the activity of dysopsonins in the serum. Biochim Biophys Acta. 1993;1179(2):157-65.

41 Sekar V, Kestens D, Spinosa-Guzman S, De Pauw M, De Paepe E, Vangeneugden T, et al. The effect of different meal types on the pharmacokinetics of darunavir (TMC114)/ritonavir in HIV-negative healthy volunteers. J Clin Pharmacol. 2007;47(4):479-84. doi: 10.1177/0091270006298603.

42 Diker B, Janneh O, van Heeswijk RP, Copeland KF. Comparative efflux of saquinavir, ritonavir and lopinavir from primary human cells. Drug Metab Lett. 2010;4(4):241-5.

43 Yan F, Zhang C, Zheng Y, Mei L, Tang L, Song C, et al. The effect of poloxamer 188 on nanoparticle morphology, size, cancer cell uptake, and cytotoxicity. Nanomed. 2010;6(1):170-8. doi: 10.1016/j.nano.2009.05.004.